



# A Complex Dynamical Study of Spatiotemporal Plankton-Fish Interaction with Effects of Harvesting

Surabhi Pareek<sup>1</sup> · Randhir Singh Baghel<sup>1</sup>

Received: 3 September 2023 / Accepted: 24 November 2023 / Published online: 30 December 2023  
© The Author(s), under exclusive licence to Shiraz University 2023

## Abstract

In this article, we propose an aquatic system, in terms of three dimensional plankton-fish interaction model that takes into account holling type II and IV functional responses. Both species (fish and phytoplankton) are thought to be growing logistically. Our objective is to apply the dynamical behavior model with constant rate harvesting to the fish population. The stability of the model system has been investigated for both geographical and non-spatial systems, and the theoretical findings have been proven using numerical simulation. It is observed that the aquatic system is particularly sensitive to maximum per capita predation rate and capable of causing bifurcating occurrences. Persistence and permanence are discussed. We observed the Hopf bifurcation situations for varied maximal per capita predation rates and harvesting constant rates. Furthermore, the diffusion-driven Turing instability is investigated, and various time level and harvesting constant rate based Turing patterns are observed. The results of this study reveal that the mortality rate of phytoplankton and the continual harvesting of the fish population play key roles in marine systems.

**Keywords** Plankton-fish model · Holling type-II and Holling type-IV functional response · Hopf bifurcation · Persistence and permanence · Harvesting yield · Diffusion · Pattern

## 1 Introduction

Mathematical modelling is a process of creating a mathematical representation of real world systems using math formulas and description. Dhar and Baghel (2016), Baghel and Dhar (2014), Baghel et al. (2012), Holt (2002), Nath et al. (2019), Kumar and Kumari (2021), Kumari and Upadhyay (2020), Maionchi et al. (2006), Callahan and Knobloch (1999). Mathematical modelling gives precision and strategy for problem solutions. It also allows better design and control of a system (Baghel et al. 2012).

Mathematical modelling of ecosystem was started by lotka and volterra. The biological or ecological interaction can be explained as pre-predation and so on (Hritonenko et al. 1999; Baghel 2023). In prey-predator system many

factors involved one of them is functional response. According to behaviour of populations, functional response has been developed (Hastings and Powell 1991). Many researchers have been used two-species models, but the interaction of three or more species may be critical to community function (Huisman and De Boer 1997).

Holling type functional responses have been performed by many researchers. The Holling type II and Holling type IV functional Responses are simple in terms of mathematically and mechanistically. Higher order models are allowed in holling type functional responses. Many researchers included mathematical model of a syn eco-symbiotic population with a prey and two predators with mutualism between the predators (Reddy and Pattabhira-macharyulu 2011).

Diffusion is vital in ecosystems, patterns arise as a result of reaction-diffusion equations and Turing instability defines how patterns appear in nature. It occurs when a homogeneous stable steady state becomes unstable in the presence of diffusion (which contradicts the general idea that diffusion is a stabilizing process). A food web model with diffusion have used by most of the authors (Upadhyay

✉ Randhir Singh Baghel  
randhir.baghel@poornima.edu.in  
Surabhi Pareek  
surabhi.pareek@poornima.edu.in

<sup>1</sup> Department of Mathematics, Poornima University, Jaipur, Rajasthan 303905, India

et al. 2011a, b; Thakur 2015; Upadhyay and Naji 2009; Bera et al. 2016).

In the spatiotemporal system The diffusion driven instability is performed (Rai and Upadhyay 2004; Zhao and Lv 2009; Upadhyay et al. 2010; Baghel et al. 2012). A mathematical model with harvesting on prey and predator both species is formulated and analyzed. The exploitation of biological resources and the harvest of population species are used in fisheries and wildlife management (Callahan and Knobloch 1999; Dhar et al. 2012; Misra et al. 2019). The predator–prey model is considered in which predator species are harvested independently with constant rates (Baghel et al. 2011; Dhar et al. 2015). Harvesting is a common and natural phenomenon. In fishery harvesting is used frequently as the biological resources are mostly renewable resources. On an exploited fishery system with interacting prey and predator species, many researchers are considering harvesting on either prey species or predator species or harvesting on both prey and predator species (Das and Pal 2019; Dubey et al. 2018; Chakraborty et al. 2015).

A fishing system with interacting predator and prey provides an intriguing scenario. The scientific communities have been exploring the harvesting of the species (Walters et al. 2016; Whipple et al. 2000; Soudijn et al. 2021).

Some authors studied a model system in order to figure out how optimal harvesting policies can be developed so that economic gain is balanced against the ecological health of the exploited system (Upadhyay and Tiwari 2017). Some authors suggested stochastic behavior of the system (Badawi et al. 2022, 2023a, b; Maayah et al. 2022).

In this work, plankton–fish model system is considered with Holling types functional responses (i.e. Holling types II and IV functional response). In Sect. 2, proposed the spatial model and 3 is non-spatial model, in this, we will obtain boundedness and the stability for interior equilibrium point. Moreover, existence of Hopf bifurcation is explained. After this, persistence and permanence are also performed. In Sect. 4, Spatiotemporal model is performed. Stability of bifurcating periodic solutions is shown and Turing instability and pattern formation are performed. Finally, conclusion is given.

## 2 Spatial Model System

An aquatic environment is home to a diverse range of water-dependent living organisms, such as plants, animals, and bacteria. The following assumptions were used to develop the aquatic model, in order to introduce spatial variations a three dimensional plankton–fish model is discussed. We have considered Holling type functional responses, where phytoplankton, zooplankton and fish

population densities are represented by  $P(T)$ ,  $Z(T)$  and  $F(T)$  (at time  $T$ ) respectively. Phytoplankton is growing logistically with growth rate  $r$  and carrying capacity  $K$ . We have used Holling type II and Holling type IV functional response. Holling type II functional response is given by  $\frac{ZF}{K_1+Z}$  and  $\frac{cPZ}{\frac{P^2}{i}+P+a}$  represents Holling type IV functional response. Table 1 contains descriptions of the remaining parameters.

Therefore, we use diffusion terms in system, the reaction-diffusion system in a bounded domain  $\Theta \subset R^3$  has been shown as below:

$$\frac{\partial P}{\partial T} = rP \left(1 - \frac{P}{K}\right) - \frac{cPZ}{\frac{P^2}{i} + P + a} + \delta_1 \Delta P \quad (1)$$

$$\frac{\partial Z}{\partial T} = \frac{cPZ}{\frac{P^2}{i} + P + a} - d_1 Z - \frac{r_1 ZF}{K_1 + Z} + \delta_2 \Delta Z \quad (2)$$

$$\frac{\partial F}{\partial T} = sF \left(1 - \frac{F}{K_2}\right) + \frac{r_2 ZF}{K_1 + Z} - hF + \delta_3 \Delta F \quad (3)$$

Initial conditions are as below:

$$P(\mu, 0) > 0, Z(\mu, 0) > 0, F(\mu, 0) > 0,$$

$$\mu = (x, y) \in \Theta.$$

subject to boundary conditions:

$\frac{\partial P}{\partial \nu} = \frac{\partial Z}{\partial \nu} = \frac{\partial F}{\partial \nu} = 0, \nu \in \partial \Theta, T > 0$ , where,  $\nu$  denotes unit normal vector of the boundary  $\partial \Theta$ .  $\delta_1$ ,  $\delta_2$  and  $\delta_3$  are diffusion coefficients for phytoplankton, zooplankton and fish population respectively.  $\Delta$  is Laplacian operator given by  $\frac{\partial^2}{\partial x^2}$  in one dimensional spatial domain and  $\frac{\partial^2}{\partial x^2} + \frac{\partial^2}{\partial y^2}$  in two dimensional spatial domain.

A brief description of parameters is as below:

## 3 Non-spatial Model system

A three dimensional plankton fish model is discussed. Where  $P(T)$ ,  $Z(T)$  and  $F(T)$  are population densities of the phytoplankton, zooplankton and fish population at time  $T$  respectively. The model is given as below:

$$\frac{dP}{dT} = rP \left(1 - \frac{P}{K}\right) - \frac{cPZ}{\frac{P^2}{i} + P + a} \quad (4)$$

$$\frac{dZ}{dT} = \frac{cPZ}{\frac{P^2}{i} + P + a} - d_1 Z - \frac{r_1 ZF}{K_1 + Z} \quad (5)$$

$$\frac{dF}{dT} = sF \left(1 - \frac{F}{K_2}\right) + \frac{r_2 ZF}{K_1 + Z} - hF \quad (6)$$

Subject to initial conditions:

$$P(0) > 0, Z(0) > 0, F(0) > 0.$$



**Table 1** Parameters used in model system are given as follows:

Parameters	Meaning
$r$	Growth rate of phytoplankton
$K$	Carrying capacity of phytoplankton
$d_1$	Mortality rate of zooplankton
$s$	Growth rate of fish population
$r_1, r_2$	Maximum uptake rates
$h$	Harvested with constant rate
$c$	Maximum per capita predation rate
$K_1$	Half saturation constant of zooplankton and fish population
$a$	The half-saturation constant in absence of any inhibitory effect
$i$	A direct measure of the predator’s immunity
$K_2$	Carrying capacity of fish population

### 3.1 Dynamical Behaviour of the Non-spatial Model System

In this part, dynamical behavior of the proposed model is discussed. First, we obtain equilibrium points of the system and discuss existence of these points. Moreover, we find local stability and bifurcation analysis is performed. Further, persistence and permanence are performed.

#### 3.1.1 Existence of Equilibrium Points and Linear Stability Analysis

There exist at most six equilibrium points of the system are: (i)  $E_0 = (0,0,0)$  (ii)  $E_1 = (K, 0, 0)$  (iii)  $E_2 = (0, 0, F)$  (iv)  $E_3 = (P, Z, 0)$  (v)  $E_4 = (P, 0, F)$  (vi)  $E_5 = (P^*, Z^*, F^*)$ . Now, we check the existence of equilibrium points and find the stability as follow:

- (i) The equilibrium point  $E_0 = (0,0,0)$  exists always. Then, the Jacobian matrix is given as

$$J(E_0) = \begin{bmatrix} r & 0 & 0 \\ 0 & -d_1 & 0 \\ 0 & 0 & s - h \end{bmatrix}$$

Eigen values of  $E_0$  are  $(r, -d_1, s - h)$ . Eigen value  $s - h$  is positive if  $s > h$ , negative if  $s < h$ . Then,  $E_0$  will be saddle point.

- (ii) Predator free equilibrium point is  $E_1 = (K, 0, 0)$ , exists for all parameter values. Thus, the Jacobian matrix is given as:

$$J(E_1) =$$

$$\begin{bmatrix} -r & \frac{-cZ}{\frac{K^2}{i} + K + a} & 0 \\ 0 & \frac{cZ}{\frac{K^2}{i} + K + a} - m & 0 \\ 0 & 0 & s - h \end{bmatrix}$$

The eigen value of  $E_1$  are  $-r, \frac{cZ}{\frac{K^2}{i} + K + a} - m$  and  $s - h$ . Eigen value is positive or negative if the condition  $\frac{cZ}{\frac{K^2}{i} + K + a} > m$  or  $\frac{cZ}{\frac{K^2}{i} + K + a} < m$  is satisfied and eigen value  $s - h$  is positive or negative if condition  $s > h$  or  $s < h$  is satisfied. If all the eigen values are negative then  $E_1$  is LAS otherwise unstable.

- (iii) The equilibrium point is  $E_2 = (0, 0, F)$ , exists. Thus the Jacobian matrix is given as:

$$J(E_2) = \begin{bmatrix} -r & 0 & 0 \\ 0 & -d_1 - \frac{r_1 F}{K_1} & 0 \\ 0 & \frac{r_2 F}{K_1} & s - h - \frac{2sF}{K_2} \end{bmatrix}$$

The eigen values of  $E_2$  are  $-r, -d_1 - \frac{r_1 F}{K_1}$ , and  $s - h$ . eigen value  $-(d_1 + \frac{r_1 F}{K_1})$  is positive or negative if the condition  $(d_1 + \frac{r_1 F}{K_1}) < 0$  or  $(d_1 + \frac{r_1 F}{K_1}) > 0$  is satisfied, hence  $E_2$  will be a saddle point.

- (iv) Top predator free equilibrium point  $E_3 = (P, Z, 0)$ , exists. Thus the Jacobian matrix

is given as:

$$J(E_3) = \begin{bmatrix} h_{11} & h_{12} & h_{13} \\ h_{21} & h_{22} & h_{23} \\ h_{31} & h_{32} & h_{33} \end{bmatrix}$$

where,

$$h_{11} = r - \frac{2Pr}{K} - \frac{\left[\frac{P^2}{i} + P + a\right]cZ - cPZ\left(\frac{2P}{i} + 1\right)}{\left(\frac{P^2}{i} + P + a\right)^2}$$

$$h_{12} = \frac{-cP}{\left(\frac{P^2}{i} + P + a\right)}, h_{13} = 0.$$

$$h_{21} = \frac{\left[\frac{P^2}{i} + P + a\right]cZ - cPZ\left(\frac{2P}{i} + 1\right)}{\left(\frac{P^2}{i} + P + a\right)^2}, h_{22} = \frac{-cP}{\left(\frac{P^2}{i} + P + a\right)},$$

$$h_{23} = \frac{r_1Z}{K_1 + Z}, h_{31} = 0, h_{32} = 0, h_{33} = s - h + \frac{r_2Z}{K_1 + Z}.$$

- (v) Zooplankton- population free equilibrium point  $E_4 = (P, 0, F)$ , exists. Thus the Jacobian matrix is given as:

$$J(E_4) = \begin{bmatrix} r - \frac{2Pr}{K} & \frac{cP}{\left(\frac{P^2}{i} + P + a\right)} & 0 \\ 0 & \frac{cP}{\left(\frac{P^2}{i} + P + a\right)} - d_1 & 0 \\ 0 & \frac{r_1F}{k_1} & s - h \end{bmatrix}$$

The eigenvalues of  $E_4$  are  $2r - \frac{2Pr}{K}, \frac{cP}{\left(\frac{P^2}{i} + P + a\right)} - d_1$  and  $s - h$ . These eigen values are negative if  $2r < \frac{2Pr}{K}, \frac{cP}{\left(\frac{P^2}{i} + P + a\right)} < d_1$  and  $s < h$ . Hence  $E_4$  will be a LAS otherwise unstable.

- (vi) The interior equilibrium point  $E_5 = (P^*, Z^*, F^*)$ , the Jacobian matrix is given as:

$$J(E_5) = \begin{bmatrix} g_{11} & g_{12} & g_{13} \\ g_{21} & g_{22} & g_{23} \\ g_{31} & g_{32} & g_{33} \end{bmatrix}$$

$$g_{11} = r - \frac{2Pr}{K} - \frac{\left[\frac{P^2}{i} + P + a\right]cZ - cPZ\left(\frac{2P}{i} + 1\right)}{\left(\frac{P^2}{i} + P + a\right)^2}$$

$$g_{12} = \frac{-cP}{\left(\frac{P^2}{i} + P + a\right)}, g_{13} = 0$$

$$g_{21} = \frac{\left[\frac{P^2}{i} + P + a\right]cZ - cPZ\left(\frac{2P}{i} + 1\right)}{\left(\frac{P^2}{i} + P + a\right)^2}$$

$$g_{22} = \frac{cP}{\left(\frac{P^2}{i} + P + a\right)} - d_1, g_{23} = \frac{-r_1Z}{(k_1 + Z)^2}$$

$$g_{31} = 0, g_{32} = \frac{K_1 r_2 F}{(k_1 + Z)^2} - \frac{K_1 r F}{(k_1 + Z)^2}$$

$$g_{33} = s - \frac{2sF}{K_2} + \frac{r_2Z}{k_1 + Z} - h$$

**Theorem 1** Assume that

$$r < -\frac{2Pr}{K} - \frac{\left[\frac{P^2}{i} + P + a\right]cZ - cPZ\left(\frac{2P}{i} + 1\right)}{\left(\frac{P^2}{i} + P + a\right)^2} \tag{7}$$

$$s + \frac{r_2Z}{k_1 + Z} < -\frac{2sF}{K_2} - h \tag{8}$$

Then the equilibrium point  $E_5(P^*, Z^*, F^*)$  is locally asymptotically stable.

**Proof** The characteristics equation is

$$\lambda^3 + A_1\lambda^2 + A_2\lambda + A_3 = 0$$

where,

$$A_1 = -(g_{11} + g_{22} + g_{33})$$

$$A_2 = g_{22}g_{33} - g_{23}g_{32} + g_{11}g_{33} + g_{11}g_{22} - g_{12}g_{21}$$

$$A_3 = g_{11}g_{23}g_{32} + g_{12}g_{21}g_{33} - g_{11}g_{22}g_{33}.$$

Now,  $E_5$  is locally asymptotically stable according to Routh–Hurwitz criterion. Clearly, we find that  $g_{11} < 0$  and  $g_{33} < 0$ . Now we can say that interior equilibrium point  $E_5(P^*, Z^*, F^*)$  of system is locally asymptotically stable. □

### 3.1.2 Hopf-bifurcation of Non-spatial System

Hopf-bifurcation happens in the system when it becomes unstable and periodic solutionaries appear in the system. We may comprehend the presence of the Hopf bifurcation by demonstrating the theorem, in which the bifurcation parameter  $\sigma$  represents the carrying capacity of the prey.

**Theorem 2** When carrying capacity  $\sigma$  of prey, crosses a critical value  $\sigma^*$ , then the Hopf-bifurcation occurs in model system (4)–(6) around the positive equilibrium  $e_5 = (P^*, Z^*, F^*)$  if the following conditions hold:

$$M_1(\sigma^*) > 0, M_3(\sigma^*) > 0, M_1(\sigma^*)M_2(\sigma^*) - M_3(\sigma^*) = 0$$

and

$$[M_1(\sigma^*)M_2(\sigma^*)]' \neq M_3'(\sigma^*).$$

**Proof** It is clear that the equilibrium point  $e_5$  is LAS and system become unstable when we change in some parameter value. We take  $\sigma$  as the bifurcation parameter. If there exists a critical value  $\sigma^*$  such that

$$M_1(\sigma^*)M_2(\sigma^*) - M_3(\sigma^*) = 0$$

For  $\sigma = \sigma^*$  the characteristic equation is given as:

$$(\lambda^2(\sigma^*) + M_2(\sigma^*))(\lambda(\sigma^*) + M_1(\sigma^*)) = 0 \tag{9}$$

Roots of above equation are:  $-M_1(\sigma^*)$ ,  $\iota\sqrt{M_2(\sigma^*)}$  and  $-\iota\sqrt{M_2(\sigma^*)}$ . If transversality condition  $\frac{Re(\lambda_i(K))}{dK}|_{\sigma=\sigma^*} \neq 0$  hold, we can say Hopf-bifurcation occurs at  $\sigma = \sigma^*$ . For all  $\sigma$ , general form of roots are

$$\begin{aligned} \lambda_1(\sigma) &= u(\sigma) + \iota v(\sigma), \\ \lambda_2(\sigma) &= u(\sigma) + \iota v(\sigma), \\ \lambda_3(\sigma) &= -M_1(\sigma). \end{aligned}$$

Substituting into (9), we get

$$Q(\sigma)u'(\sigma) - U(\sigma)v'(\sigma) + V(\sigma) = 0, \tag{10}$$

$$U(\sigma)u'(\sigma) + Q(\sigma)v'(\sigma) + W(\sigma) = 0, \tag{11}$$

Where,

$$\begin{aligned} Q(\sigma) &= 3u^2(\sigma) + 2M_1(\sigma)u(\sigma) + M_2(\sigma) - 3v^2(\sigma) \\ U(\sigma) &= 6u(\sigma)v(\sigma) + 2M_1v(\sigma) \\ V(\sigma) &= u^2(\sigma)M'_1(\sigma) + M'_2u(\sigma) + M'_3(\sigma) - M'_1(\sigma)v^2(\sigma) \\ W(\sigma) &= 2u(\sigma)v(\sigma)M'_1(\sigma) + M'_2(\sigma)v(\sigma) \end{aligned}$$

Here,  $u(\sigma) = 0$ ,  $v(\sigma) = \sqrt{M_2(\sigma^*)}$ , we get

$$Q(\sigma^*) = -2M_2(\sigma^*), \quad U(\sigma^*) = 2M_1(\sigma^*)\sqrt{M_2(\sigma^*)},$$

$$V(\sigma^*) = M'_3(\sigma^*) - M'_1(\sigma^*)M_2(\sigma^*),$$

$$W(\sigma^*) = M'_2(\sigma^*)\sqrt{M_2(\sigma^*)}$$

Solving  $u'(\sigma^*)$  from Eqs. (10) and (11) we get,

$$\frac{Re(\lambda_i(\sigma))}{d\sigma}|_{\sigma=\sigma^*} = u'(\sigma)|_{\sigma=\sigma^*} = -\frac{U(\sigma^*)W(\sigma^*) + Q(\sigma^*)V(\sigma^*)}{Q^2(\sigma^*) + L^2(\sigma^*)} = \frac{1}{2}$$

$$\frac{M'_3(\sigma^*) - (M_1(\sigma^*)M_2(\sigma^*))'}{M_1^2(\sigma^*) + M_2(\sigma^*)} \neq 0$$

If  $(M_1(\sigma^*)M_2(\sigma^*))' \neq M'_3(\sigma^*)$  and

$$\lambda_3(\sigma^*) = -M_1(\sigma^*) < 0$$

Hence the theorem is proved. Because transversality conditions hold and we can say that Hopf-bifurcation occurs at  $\sigma = \sigma^*$ . Hence the theorem is established.

Here, we take certain parameter values  $r = 2$ ,  $K = 0.01$ ,  $m = 0.1$ ,  $r_1 = 0.3$ ,  $s = 0.02$ ,  $a = 0.01$ ,  $i = 2$ ,  $K_1 = 0.054$ ,  $K_2 = .02$ ,  $r_2 = 0.03$ ,  $h = 0.01$ .

The system (4)–(6) is stable at the coexistence equilibrium point  $E^*$ , which is depicted with the time series and phase space diagram of system (4)–(6) in Figs. 1, 4, and 6, if we assume  $c = 1.6$  and  $h = 1$ . We now view the system from the other perspective. The system becomes unstable and oscillates around the coexistence equilibrium point  $E^*$  if we select  $c = 2.22$  and  $h = 0.8$ . The phase space diagram and time series of system (4)–(6) are depicted in Figs. 2, 3, 5, and 7.

Figures 4, 6 illustrate the stability areas of the system in the PZ and ZF-plane, where the system exhibits stable dynamics and Figs. 5, 7 illustrate the system’s dynamics in the PZ and ZF-plane, where the system exhibits unstable dynamics.  $\square$

The impact of harvesting constant rate on  $h = 0.8$  is demonstrated here to exhibit oscillatory behavior (see Fig. 6), whereas  $h = 1$  exhibits steady behavior (see Fig. 7).

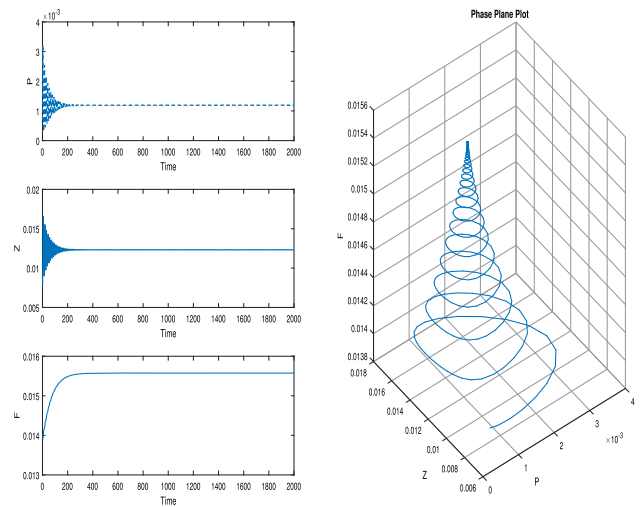


Fig. 1 Time series, phase portrait for the system (4)–(6) at  $c = 1.6$

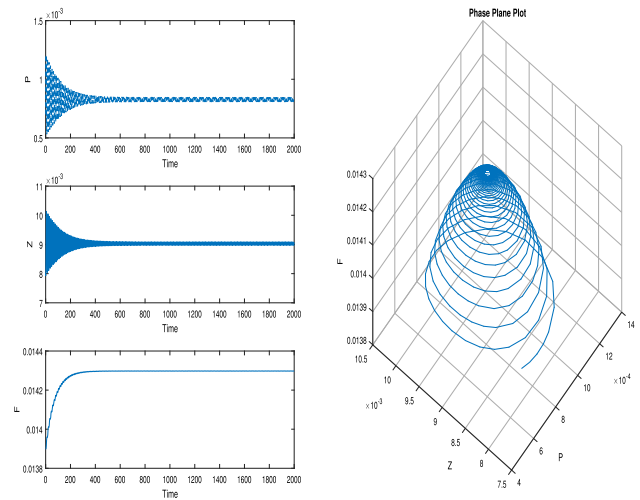


Fig. 2 Time series, phase portrait for the system (4)–(6) at  $c = 2.22$

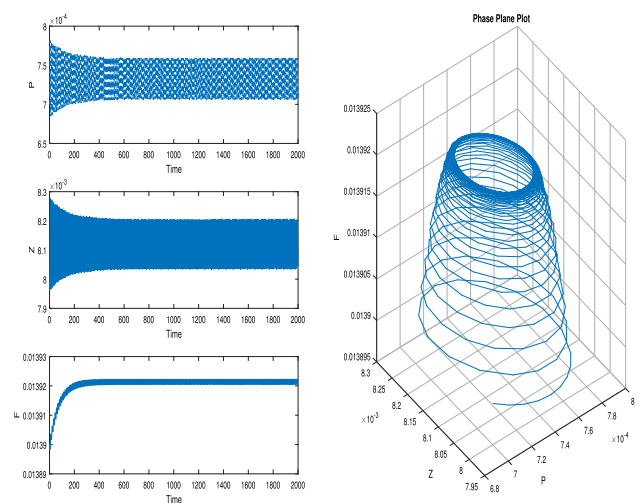


Fig. 3 Time series, phase portrait the system (4)–(6) at  $c = 2.45$

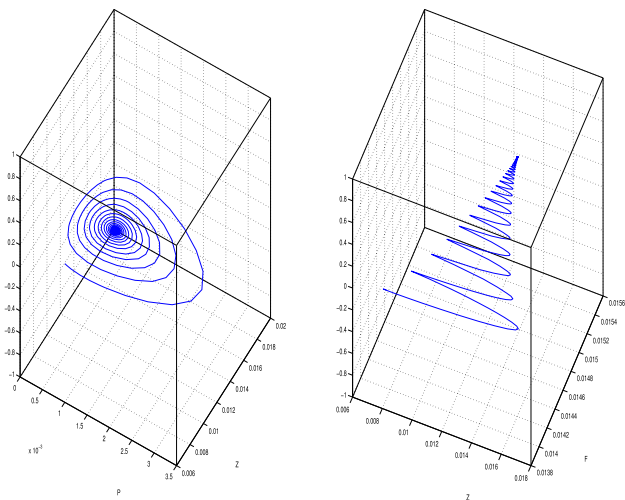


Fig. 4 Phase portraits of the system (4)–(6) for a stable limit cycle at  $c = 1.6$

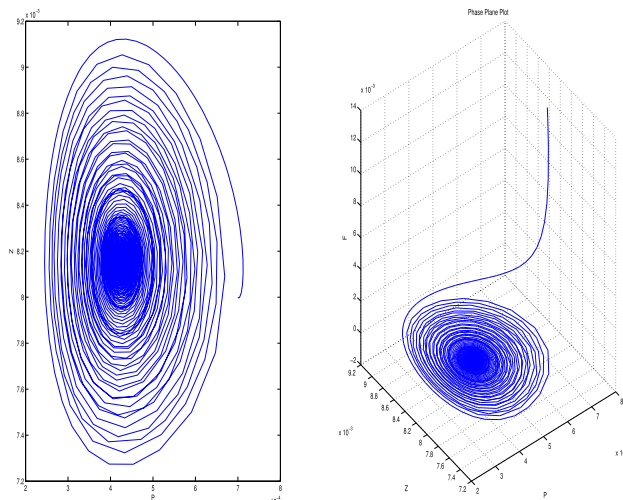


Fig. 6 Phase portraits of the system (4)–(6) for a stable limit cycle at  $h = 1$

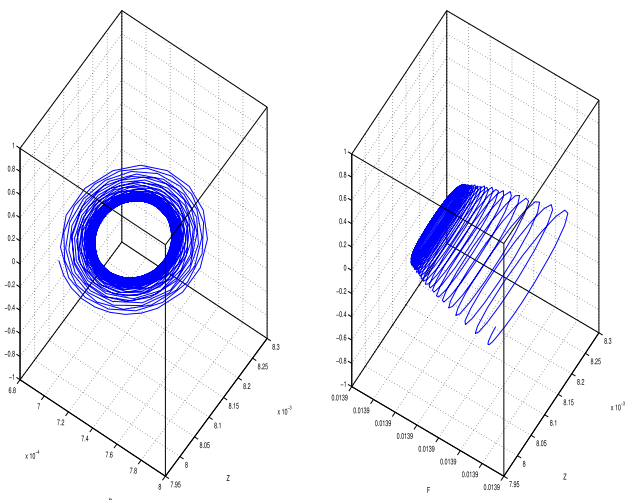


Fig. 5 Phase portraits of the system (4)–(6) for an unstable limit cycle at  $c = 2.45$

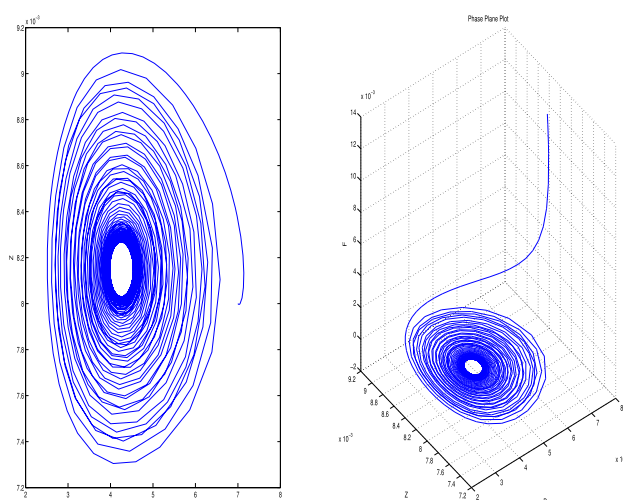


Fig. 7 Phase portraits of the system (4)–(6) for an unstable limit cycle at  $h = 0.8$

### 3.1.3 Persistence and Permanence

The permanence of a system indicates that strictly positive solutions do not have omega limit points on the border of the non-negative cone. Persistence and permanence are crucial system behaviors for understanding the system’s long-term behavior.

**Theorem 3** *All the solutions of the model system which start in  $R^3_+$  are uniformly bounded.*

**Proof** Let  $(P(T), Z(T), F(T))$  be any solution of the model with positive initial condition.

Now, we consider a function  $\phi(P, Z, T) = P + Z + \frac{r_1}{r_2}F$ . Then differentiating above function with respect to T, we have

$$\frac{d\phi}{dT} = \frac{dP}{dT} + \frac{dZ}{dT} + \frac{r_1}{r_2} \frac{dF}{dT}$$

Putting the values of  $P(T), Z(T)$  and  $F(T)$ , we get

$$\frac{d\phi}{dT} = rP\left(1 - \frac{P}{K}\right) - d_1Z + \frac{sFr_1}{r_2}\left(1 - \frac{F}{K_2}\right) - \frac{hr_1F}{r_2}.$$

Then we have the following differential equation:

$$\frac{d\phi}{dT} + \eta\phi \leq \frac{K(r+\eta)^2}{4r} + \frac{r_1K_2(s+\eta)^2}{4r_2s} - Z(d_1 - \eta)$$

Now, we define  $\eta < d_1$ , then above inequality is bounded

by  $\frac{K(r+\eta)^2}{4r} + \frac{r_1K_2(s+\eta)^2}{4r_2s}$ . Thus we find  $l > 0$ , such that

$$\frac{d\phi}{dT} + \eta\phi \leq l, \text{ which conclude that}$$

$$\phi(T) \leq \phi(0)e^{-\eta T} + \frac{l}{\eta}(1 - e^{-\eta T}) \leq \max(\phi(0), \frac{l}{\eta}).$$

Hence, All the solutions of the model system (1) are uniformly bounded. Theorem is proved.  $\square$

**Theorem 4** *The model system (4)–(6) is uniformly persistent if conditions are satisfied as below:*

$$r\eta_1 > d_1\eta_2 + (h - s)\eta_3$$

$$\eta_2 > \frac{(h-s)\eta_3}{\left(\frac{cK}{\frac{p^2}{t}+k+a} - d_1\right)}$$

$$s + \frac{r_2Z}{K_1+Z} > h$$

**Proof** Let  $\zeta(P, Z, F) = P^{\eta_1}Z^{\eta_2}F^{\eta_3}$  be lyapunov function.

Taking log both the sides and differentiating, we get

$$\psi(P, Z, F) = \frac{\dot{\zeta}}{\zeta} = \eta_1 \left[ r \left( 1 - \frac{P}{K} \right) - \frac{cZ}{\frac{p^2}{t}+P+a} \right]$$

$$+ \eta_2 \left[ \frac{cP}{\frac{p^2}{t}+P+a} - d_1 - \frac{r_1F}{K_1+Z} \right] + \eta_3 \left[ s \left( 1 - \frac{F}{K_2} \right) + \frac{r_2Z}{K_1+Z} - h \right].$$

$\psi(P, Z, F) > 0$  is enough condition to prove the uniform persistence of the system. Following are conditions for the system to be uniformly persistent.

$$\psi(0, 0, 0) = \eta_1 r - d_1\eta_2 + \eta_3(s - h) > 0$$

$$\psi(K, 0, 0) = \eta_2 \frac{cK}{\frac{p^2}{t}+K+a} - d_1\eta_2 + s\eta_3 - h\eta_3 > 0$$

$$\psi(P, Z, 0) = \eta_1 \left[ r \left( 1 - \frac{P}{K} \right) - \frac{cZ}{\frac{p^2}{t}+P+a} \right] + \eta_2 \left( \frac{cP}{\frac{p^2}{t}+P+a} - d_1 \right)$$

$$+ \eta_3 \left[ s + \frac{r_2Z}{K_1+Z} - h \right] = s - h + \frac{r_2Z}{K_1+Z} > 0$$

These conditions are satisfied if the conditions stated in theorem holds.  $\square$

### 3.1.4 Maximum Harvesting Yield (MSY)

The growth of fish population depends on zooplankton for complete model system and we obtain

$$h = sF \left( 1 - \frac{F}{K_2} \right) + \frac{r_2ZF}{K_1+Z}$$

where h represents the reduction in fish population due to harvesting.

So,  $\frac{\partial h}{\partial F} = 0$ , which gives  $F = \frac{K_2}{2s} \left( s + \frac{r_2Z}{K_1+Z} \right)$ , where  $\frac{K_2}{2s} \left( s + \frac{r_2Z}{K_1+Z} \right) > 0$  and  $\frac{\partial^2 h}{\partial F^2} = \frac{-2s}{K_2} < 0$ . Thus we have

$$h_{MSY} = \frac{K_2s}{4} \left[ 1 + \frac{r_2Z}{s(K_1+Z)} \right]^2$$

Hence, we have a maximum sustainable yield when  $h_{MSY} = \frac{K_2s}{4}$ . Also,  $h > h_{MSY}$ , and  $h < h_{MSY}$  indicate, respectively, the over- and under-exploitation of the fish population.

## 4 Dynamical Behaviour of the Spatial Model System

In this section, linear stability is discussed. The spatial system about the equilibrium point  $(P^*, Z^*, F^*)$  has been linearized for this purpose, and the system has been disturbed as follows:

$$P(T, x, y) = P^* + \hat{P}(T, x, y), \tag{12}$$

$$Z(T, x, y) = Z^* + \hat{Z}(T, x, y), \tag{13}$$

$$F(T, x, y) = F^* + \hat{F}(T, x, y) \tag{14}$$

Here,  $\hat{P}, \hat{Z}, \hat{F}$  are small perturbations of time and space.

$$\hat{P} = \epsilon_1 \exp(\lambda_\sigma T) \cos(\sigma_x x) \cos(\sigma_y y),$$

$$\hat{Z} = \epsilon_2 \exp(\lambda_\sigma T) \cos(\sigma_x x) \cos(\sigma_y y),$$

$$\hat{F} = \epsilon_3 \exp(\lambda_\sigma T) \cos(\sigma_x x) \cos(\sigma_y y),$$

Here,  $\epsilon_1, \epsilon_2, \epsilon_3$  are positive and sufficiently small constants.  $\sigma_x$  and  $\sigma_y$  are components of wave number  $\sigma = \sqrt{\sigma_x^2 + \sigma_y^2}$  along x and y directions respectively and  $\lambda_\sigma$  is wavelength.

Now, we have:

$$\frac{\partial \hat{P}}{\partial T} = d_{11}\hat{P} + d_{12}\hat{Z} + d_{13}\hat{F} + \delta_1\Delta\hat{P},$$

$$\frac{\partial \hat{Z}}{\partial T} = d_{21}\hat{P} + d_{22}\hat{Z} + d_{23}\hat{F} + \delta_2\Delta\hat{Z},$$

$$\frac{\partial \hat{F}}{\partial T} = d_{31}\hat{P} + d_{32}\hat{Z} + d_{33}\hat{F} + \delta_3\Delta\hat{F},$$

The Jacobian matrix of linearized system is:

$$\begin{bmatrix} d_{11} - \delta_1\sigma^2 & d_{12} & 0 \\ d_{21} & d_{22} - \delta_2\sigma^2 & d_{23} \\ 0 & d_{32} & d_{33} - \delta_3\sigma^2 \end{bmatrix}$$

where,

$$d_{11} = r - \frac{2Pr}{K} - \frac{\left[ \frac{p^2}{t} + P + a \right] cZ - cPZ \left( \frac{2P}{t} + 1 \right)}{\left( \frac{p^2}{t} + P + a \right)^2}$$

$$d_{12} = \frac{-cP}{\left( \frac{p^2}{t} + P + a \right)}, d_{13} = 0$$

$$d_{21} = \frac{\left[ \frac{p^2}{t} + P + a \right] cZ - cPZ \left( \frac{2P}{t} + 1 \right)}{\left( \frac{p^2}{t} + P + a \right)^2}$$

$$d_{22} = \frac{cP}{\left( \frac{p^2}{t} + P + a \right)} - d_1, d_{23} = \frac{-r_1Z}{(k_1+Z)^2}$$

$$d_{31} = 0, d_{32} = \frac{K_1r_2F}{(k_1+Z)^2} - \frac{K_1rF}{(k_1+Z)^2}$$

$$d_{33} = s - \frac{2sF}{K_2} + \frac{r_2Z}{k_1+Z} - h$$

The characteristic equation corresponding to the Jacobian matrix is written as below:

$$\lambda_\sigma^3 + a_1(\sigma^2)\lambda_\sigma^2 + a_2(\sigma^2)\lambda_\sigma + a_3(\sigma^2) = 0,$$

Here,

$$a_1(\sigma^2) = \sigma^2(\delta_1 + \delta_2 + \delta_3) + E_1$$

$$a_2(\sigma^2) = \sigma^4(\delta_1\delta_2 + \delta_1\delta_3 + \delta_2\delta_3) - \sigma^2((\delta_2(d_{11} + d_{33}) + \delta_1(d_{22} + d_{33} + \delta_3(d_{11} + d_{22})))) + E_2$$

$$a_3(\sigma^2) = \delta_1\delta_2\delta_3\sigma^6 - \sigma^4(\delta_2\delta_3d_{11} + \delta_1\delta_3d_{22} + \delta_1\delta_2d_{33}) + \sigma^2(\delta_1(d_{22}d_{33} - d_{23}d_{32}) + \delta_2d_{11}d_{33} + \delta_3(d_{11}d_{22} - d_{12}d_{21})) + E_3,$$

with

$$E_1 = -(d_{11} + d_{22} + d_{33}),$$

$$E_2 = d_{22}d_{33} - d_{23}d_{32} + d_{11}d_{33} + d_{11}d_{22} - d_{12}d_{21},$$

$$E_3 = d_{11}d_{23}d_{32} + d_{12}d_{21}d_{33} - d_{11}d_{22}d_{33},$$

and

$$a_1(\sigma^2)a_2(\sigma^2) - a_3(\sigma^2) = u_0 + u_1(\sigma^2) + u_2(\sigma^4) + u_3(\sigma^6),$$

where

$$u_0 = E_1E_2 - E_3, \quad u_1 = E_2(\delta_1 + \delta_2 + \delta_3) - E_1(\delta_2(d_{33} + d_{11}) + \delta_3(d_{22} + d_{11})) + \delta_1(d_{22} + d_{33}) - \delta_1(d_{22}d_{33} - d_{23}d_{32}) - \delta_2(d_{33}d_{11}) - \delta_3(d_{22}d_{11} - d_{12}d_{21}),$$

$$u_2 = d_{11}\delta_2\delta_3 + d_{22}\delta_1\delta_3 + d_{33}\delta_1\delta_2 + E_1(\delta_1\delta_2 + \delta_1\delta_3 + \delta_2\delta_3 - (\delta_1 + \delta_2 + \delta_3)(\delta_1(d_{33} + d_{11}) + \delta_3(d_{22} + d_{11}) + \delta_1(d_{22} + d_{33}))),$$

$$u_3 = (\delta_1 + \delta_2 + \delta_3)(\delta_1\delta_2 + \delta_1\delta_3 + \delta_2\delta_3) - \delta_1(d_{22}d_{33} - d_{23}d_{32}).$$

Hence from the Routh–Hurwitz criterion, spatial system is stable if

$$a_1(\sigma^2) > 0, a_3(\sigma^2) > 0, a_1(\sigma^2)a_2(\sigma^2) - a_3(\sigma^2) > 0. \tag{15}$$

**Theorem 5** *If the positive equilibrium point  $(P^*, Z^*, F^*)$  is LAS for temporal model system(4)–(6), then  $(P^*, Z^*, F^*)$  is LAS for spatiotemporal model system (1)–(3).*

**Proof** The proof of above theorem follows from Routh–Hurwitz criterion, hence omitted.  $\square$

### 4.1 Hopf-Bifurcation of Spatial Model System

Now, here the existence of hopf bifurcation for spstial model is discussed with equilibrium point  $\hat{P} = P - P^*, \hat{Z} = Z - Z^*, \hat{F} = F - F^*$ .

Then the system becomes:

$$\frac{\partial P}{\partial T} = r(P + P^*) \left( 1 - \frac{(P + P^*)}{K} \right) - \frac{c(P + P^*)(Z + Z^*)}{\frac{(P+P^*)^2}{i} + (P + P^*) + a} + \delta_1 \Delta P \tag{16}$$

$$\frac{\partial Z}{\partial T} = \frac{c(P + P^*)(Z + Z^*)}{\frac{(P+P^*)^2}{i} + (P + P^*) + a} - d_1(Z + Z^*) - \frac{r_1(Z + Z^*)(F + F^*)}{K_1 + (Z + Z^*)} + \delta_2 \Delta Z \tag{17}$$

$$\frac{\partial F}{\partial T} = s(F + F^*) \left( 1 - \frac{(F + F^*)}{K_2} \right) + \frac{r_2(Z + Z^*)(F + F^*)}{K_1 + (Z + Z^*)} - h(F + F^*) + \delta_3 \Delta F \tag{18}$$

After the transformation the model system takes the form as below:

$$\dot{p}(T) = l(p) + n(p),$$

where

$$l = \begin{bmatrix} A_{100} + \delta_1 \Delta P & A_{010} & 0 \\ B_{100} & B_{010} + \delta_2 \Delta Z & B_{001} \\ 0 & C_{010} & \delta_3 \Delta F \end{bmatrix}$$

and  $n(p) = (f_1, f_2, f_3)^T$ .

Let us consider,

$$l = k_m + \delta_n \begin{bmatrix} \Delta & 0 & 0 \\ 0 & \Delta & \\ 0 & 0 & \Delta \end{bmatrix}$$

and  $n(p) = (f_1, f_2, f_3)^T$ .

Here,

$$k_m = \begin{bmatrix} A_{100} & A_{010} & 0 \\ B_{100} & B_{010} & B_{001} \\ 0 & C_{010} & 0 \end{bmatrix}$$

$$\text{and } \delta_n = \begin{bmatrix} \delta_1 & 0 & 0 \\ 0 & \delta_2 & 0 \\ 0 & 0 & \delta_3 \end{bmatrix}$$

then,

$$\dot{p}(T) = l(p),$$

Characteristic equation is given as

$$\lambda w - \delta_n \begin{bmatrix} \Delta & 0 & 0 \\ 0 & \Delta & \\ 0 & 0 & \Delta \end{bmatrix} w - k_m w = 0$$

where

$$w \in \text{dom } \delta_n \begin{bmatrix} \Delta & 0 & 0 \\ 0 & \Delta & 0 \\ 0 & 0 & \Delta \end{bmatrix}$$

The eigen value problem is:

$$-\Delta \phi = \lambda \phi, v \in \Omega$$

$$\partial \phi_v = 0, v \in \partial \Omega$$

has eigenvalues  $0 = \lambda_0 < \lambda_1 < \lambda_2 < \dots < \lambda_\sigma < \dots$ , and corresponding eigenfunctions are

$$\gamma_\sigma = \phi_\sigma(v), \sigma \in N_0 = 0, 1, 2, \dots$$

Let

$$\beta_\sigma^1 = \begin{bmatrix} \gamma_\sigma \\ 0 \\ 0 \end{bmatrix}, \beta_\sigma^2 = \begin{bmatrix} 0 \\ \gamma_\sigma \\ 0 \end{bmatrix}, \beta_\sigma^3 = \begin{bmatrix} 0 \\ 0 \\ \gamma_\sigma \end{bmatrix}.$$

Then,  $B_\sigma = (\beta_\sigma^1, \beta_\sigma^2, \beta_\sigma^3)_{\sigma=0}^\infty$  establish a basis. and

$$w \in \text{dom} \left( \delta_n \begin{bmatrix} \Delta & 0 & 0 \\ 0 & \Delta & 0 \\ 0 & 0 & \Delta \end{bmatrix} \right) - 0$$

can be formed as

$$w = \sum_{\sigma=1}^\infty (\beta_\sigma^1, \beta_\sigma^2, \beta_\sigma^3) \begin{bmatrix} \langle w, \beta_\sigma^1 \rangle \\ \langle w, \beta_\sigma^2 \rangle \\ \langle w, \beta_\sigma^3 \rangle \end{bmatrix}.$$

Characteristic equation is given as below:

$$\det \begin{bmatrix} \lambda + \delta_1 \lambda_\sigma - A_{100} & -A_{010} & 0 \\ -B_{100} & \lambda + \delta_2 \lambda_\sigma - B_{010} & -B_{001} \\ 0 & -C_{010} & \lambda + \delta_3 \lambda_\sigma \end{bmatrix}$$

for some  $\sigma \in N_0$ . Therefore,

$$\lambda^3 + \mu_1 \lambda^2 + \mu_2 \lambda + \mu_3 = 0,$$



where

$$\mu_1 = \lambda_\sigma(\delta_1 + \delta_2 + \delta_3) + E_1,$$

$$\mu_2 = \lambda_\sigma^2(\delta_1\delta_2 + \delta_2\delta_3 + \delta_3\delta_1) - \lambda_\sigma(A_{100}(\delta_2 + \delta_3) + B_{010}(\delta_1 + \delta_3)) + E_2$$

$$\mu_3 = \delta_1\delta_2\delta_3\lambda_\sigma^3 - \lambda_\sigma^2(A_{100}\delta_2\delta_3 + B_{010}\delta_3\delta_1) + \lambda_\sigma(\delta_3(A_{100}B_{010} - A_{010}B_{100}) - \delta_1B_{001}C_{010}) + E_3,$$

$$E_1 = -(A_{010} + B_{010}),$$

$$E_2 = A_{100}B_{010} - A_{010}B_{100} - B_{001}C_{010},$$

$$E_3 = A_{100}B_{001}C_{010}.$$

After some calculation we get,

$$\mu_1\mu_2 - \mu_3 = \tilde{F}_1\lambda_\sigma^3 + \tilde{F}_1\lambda_\sigma^2 + \tilde{F}_1\lambda_\sigma + E_1E_2 - E_3$$

$$(\lambda^2 + \mu_2)(\lambda + \mu_1) = 0$$

For all  $\lambda$ , general form of roots are

$$\lambda_1(h_B) = \rho_1(h_B) + i\rho_2(h_B),$$

$$\lambda_2(h_B) = \rho_1(h_B) + i\rho_2(h_B),$$

$$\lambda_3(h_B) = -\mu_1(h_B).$$

Substituting into we get

$$L_1(h_B)\rho_1'(h_B) - L_2(h_B)\rho_2'(h_B) + L_3(h_B) = 0,$$

$$L_1(h_B)\rho_2'(h_B) + L_2(h_B)\rho_1'(h_B) + L_4(h_B) = 0,$$

Where,

$$L_1(h_B) = 3\rho_1^2(h_B) + 2\mu_1(h_B)\rho_1(h_B) + \mu_2(h_B) - 3\rho_2^2(h_B)$$

$$L_2(h_B) = 6\rho_1(h_B)\rho_2(h_B) + 2\mu_1\rho_2(h_B)$$

$$L_3(h_B) = \rho_1^2(h_B)\mu_1'(h_B) + \mu_2'\rho_1(h_B) + \mu_3'(h_B) - \mu_1'(h_B)\rho_2^2(h_B)$$

$$L_4(h_B) = 2\rho_1(h_B)\rho_2(h_B)\mu_1'(h_B) + \mu_2'(h_B)\rho_2(h_B)$$

Here,  $\rho_1(h_B^*) = 0$ ,  $\rho_2(h_B^*) = \sqrt{\mu_2(h_B^*)}$ , we get

$$L_1(h_B^*) = -2\mu_2(h_B^*), \quad L_2(K^*) = 2\mu_1(h_B^*)\sqrt{\mu_2(h_B^*)},$$

$$L_3(h_B^*) = \mu_3'(h_B^*) - \mu_1'(h_B^*)\mu_2(h_B^*),$$

$$L_4(h_B^*) = \mu_2'(h_B^*)\sqrt{\mu_2(h_B^*)}$$

Solving  $\rho_1'(K^*)$ , we get:

$$\frac{Re(\lambda_i(K))}{dK} \Big|_{h_B=h_B^*} = \rho_1'(h_B)_{h_B=h_B^*} = -\frac{L_2(h_B^*)K_4(h_B^*) + L_1(h_B^*)L_3(h_B^*)}{L_1^2(h_B^*) + L_2^2(K^*)}$$

$$= \frac{1}{2} \frac{\mu_3'(h_B^*) - \mu_1'(h_B^*)\mu_2(h_B^*)}{\mu_1^2(h_B^*) + \mu_2(h_B^*)} \neq 0$$

$$\text{and } \lambda_3(h_B^*) = -\mu_1(h_B^*) < 0$$

Hence the theorem is proved. Because transversality conditions hold and we can say that Hopf-bifurcation occurs at  $h_B = h_B^*$ .

### 4.2 Turing Instability

When a system becomes unstable, Turing instability occurs. The species diffusion coefficients determine the Turing stability.

**Theorem 6** *if one of the following conditions is satisfied, Turing instability occurs in the system:*

- (i) If  $r_2 > 0$  and  $r_2^2 - 4r_1r_3 > 0$  then  $\sigma_f^2$  is positive and real.
- (ii) If  $q_2 > 0$  and  $q_2^2 - 3q_1q_3 > 0$  then  $\sigma_f^2$  is positive and real.

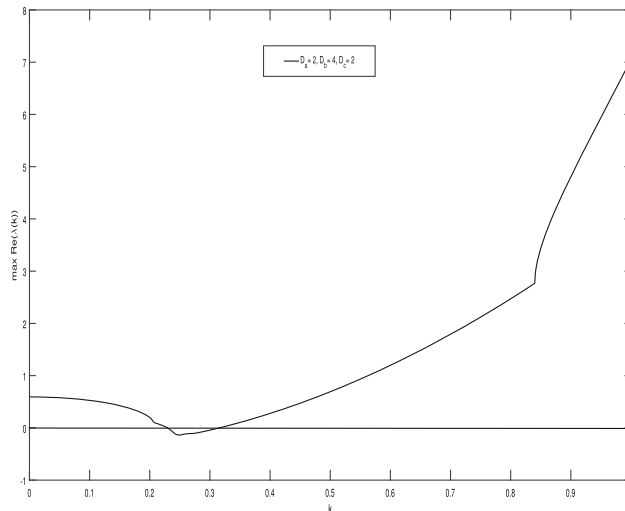


Fig. 8 Maximum  $Re(\lambda(K))$  against  $K$

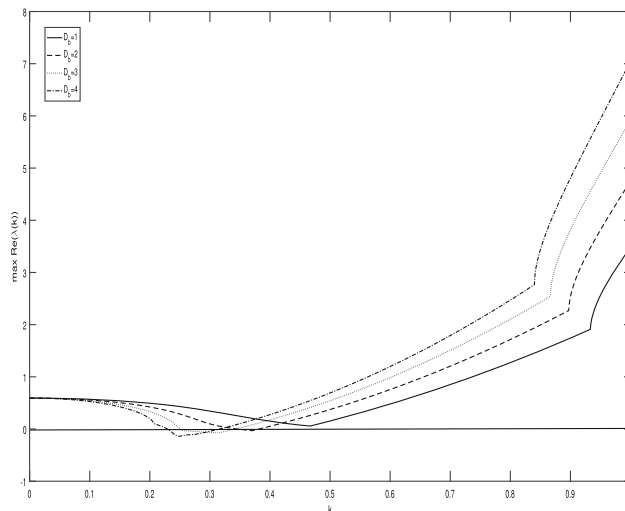


Fig. 9 Maximum  $Re(\lambda(K))$  against  $K$

- (iii) If  $a_3(\sigma_f^2) = \frac{2q_2^3 - 9q_1q_2q_3 + 27q_1^2q_4 - 2(q_2^2 - 3q_1q_3)^{\frac{3}{2}}}{27q_1^2} < 0$  and if  $u_1 < 0, u_2 < 0$ , and  $\phi(\sigma^2) = \frac{2u_1^3 - 9u_0u_1u_2 + 27u_0^2u_3 - 2(u_1^2 - 3u_0u_2)^{\frac{3}{2}}}{27u_0^2} < 0$ .

Then, the Turing instability occurs around equilibrium of the system.

**Proof**  $a_1(\sigma^2) > 0, a_3(\sigma^2) > 0, a_1(\sigma^2)a_2(\sigma^2) - a_3(\sigma^2) < 0$ .

Let us assume that  $\mu = \sigma^2$ , we have

$$a_2(\mu) = r_1\mu^2 + r_2\mu + r_3,$$

where,

$$r_1 = \delta_1\delta_2 + \delta_1\delta_3 + \delta_2\delta_3,$$

$$r_2 = -\delta_2(d_{11} + d_{33} - \delta_1(d_{22} + d_{33} - \delta_3(d_{11} + d_{22}),$$

$$r_3 = E_3.$$

It is easy to see that if  $a_2(\mu) = r_1\mu^2 + r_2\mu + r_3 < 0$  holds, then equilibrium of system become unstable.

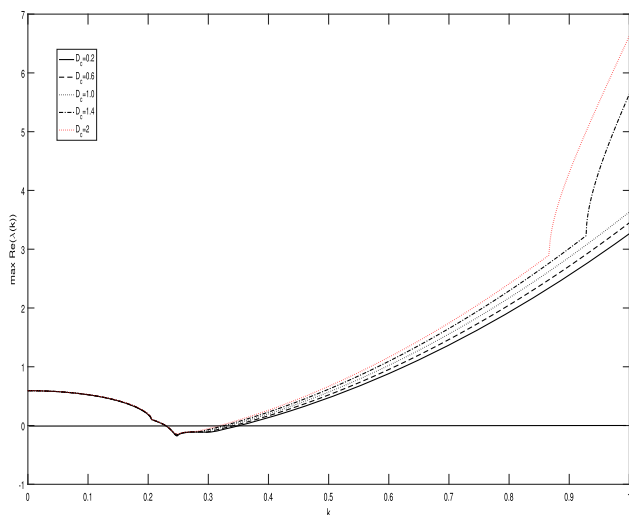


Fig. 10 Maximum  $Re(\lambda(K))$  against  $K$

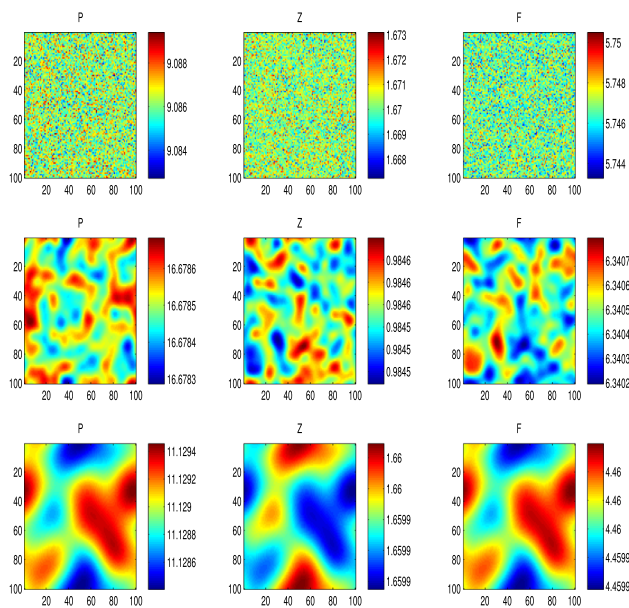


Fig. 11 Spatial distribution of phytoplankton (first column), zooplankton (second column) and fish (third column) are population densities of the spatial system (1)–(3). Spatial patterns are obtained with diffusivity coefficients  $D_a = 0.02$ ,  $D_b = 0.04$ ,  $D_c = 0.02$  and harvesting  $h = 0.01$  at different time levels: for  $T = 10$ ,  $T = 100$ ,  $T = 400$

Roots of above equation given as below:

$$\mu_{1,2} = \frac{-r_2 \pm \sqrt{r_2^2 - 4r_1r_3}}{2r_1}.$$

$r_2 > 0$  and  $r_2^2 > 4r_1r_3$  for some  $\mu$  is sufficient to show Turing instability. Turing instability occurs in the range  $\mu_1 < \sigma^2 < \mu_2$ .

Now, we have

$$a_3 = q_1\mu^3 + q_2\mu^2 + q_3\mu + q_4,$$

where

$$q_1 = \delta_1\delta_2\delta_3,$$

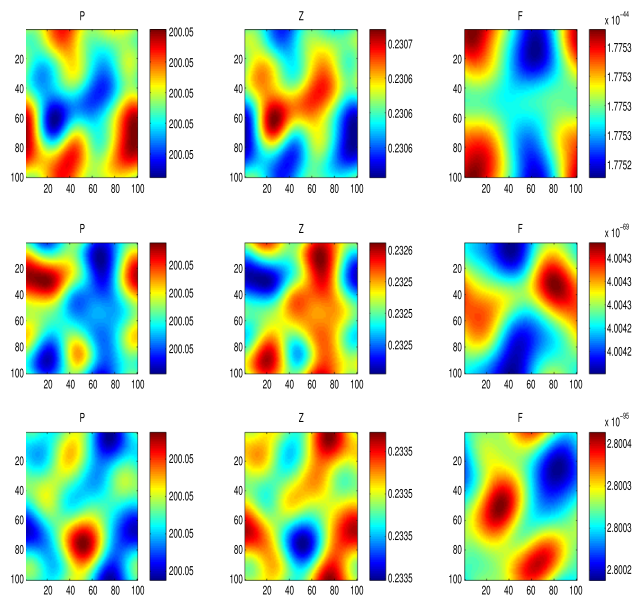


Fig. 12 Spatial distribution of phytoplankton (first column), zooplankton (second column) and fish (third column) are population densities of the spatial system (1)–(3). Spatial patterns are obtained with diffusivity coefficients  $D_a = 0.2$ ,  $D_b = 0.4$ ,  $D_c = 0.6$  and harvesting  $h = 1, 1.5, 2$  at different time levels: for  $T = 10$ ,  $T = 100$ ,  $T = 400$

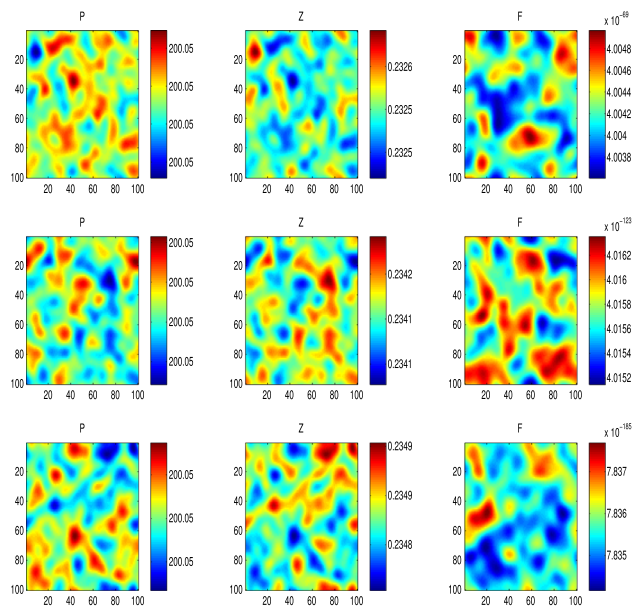
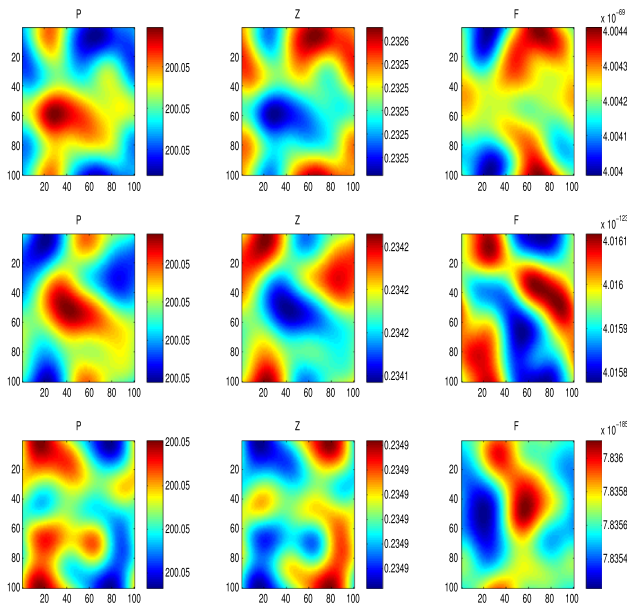


Fig. 13 Spatial distribution of phytoplankton (first column), zooplankton (second column) and fish (third column) are population densities of the spatial system (1)–(3). Spatial patterns are obtained with diffusivity coefficients  $D_a = 0.02$ ,  $D_b = 0.04$ ,  $D_c = 0.06$  and time  $T = 100$  at different harvesting values  $h = 1.5, 2.5, 3.5$

$$q_2 = -(\delta_2\delta_3d_{11} + \delta_1\delta_3d_{22} + \delta_1\delta_2d_{33}),$$

$$q_3 = \delta_1(d_{22}d_{33} - d_{23}d_{32}) + \delta_2d_{11}d_{23} + \delta_3(d_{11}d_{22} - d_{12}d_{21}),$$

$a_3$  has minima, for this purpose we need to as below:



**Fig. 14** Spatial distribution of phytoplankton (first column), zoo-plankton (second column) and fish (third column) are population densities of the spatial system (1)–(3). Spatial patterns are obtained with diffusivity coefficients  $D_a = 0.2$ ,  $D_b = 0.4$ ,  $D_c = 0.6$  and time  $T = 100$  at different harvesting values  $h = 1.5, 2.5, 3.5$

$$\frac{da_3}{d\mu} = 3q_1\mu^2 + 2q_2\mu + q_3,$$

it gives,

$$\sigma_f^2 = \frac{-q_2 + \sqrt{q_2^2 - 3q_1q_3}}{3q_1}.$$

where,  $\frac{d^2a_3}{d\mu^2} > 0$ . Hence  $p_2 > 0$  and  $q_2^2 - 3q_1q_3 > 0$ , then it is simple to verify Turing instability around equilibrium point, if

$$a_3(\sigma_f^2) = \frac{2q_3^3 - 9q_1q_2q_3 + 27q_1^2q_4 - 2(q_2^2 - 3q_1q_3)^{\frac{3}{2}}}{27q_1^3} < 0$$

For the turing instability we need to show that  $a_1(\sigma^2)a_2(\sigma^2) - a_3(\sigma^2) < 0$ .

$\sigma$  is wave number.

Now,

$$\phi(\mu) = u_0\mu^3 + u_1\mu^2 + u_2\mu + u_3,$$

where,  $u_0, u_1, u_2, u_3$  and  $E_1, E_2, E_3$  are as above.

$\phi(\sigma^2)$  is minimum at some  $\sigma^2$ ,

$$\frac{d\phi}{d\mu} = 3u_0\mu^2 + 2u_1\mu + u_2 = 0$$

where,  $\mu = \sigma^2$  and  $\frac{d^2\phi}{d\mu^2} > 0$ . Clearly,  $\phi(\sigma^2)$  has minimum at

$$\sigma_f^2 = \frac{-u_1 + \sqrt{u_1^2 - 3u_0u_2}}{3u_0}.$$

if we choose  $u_1 < 0$  and  $u_2 < 0$ , if condition

$$\phi(\sigma^2) = \frac{2u_1^3 - 9u_0u_1u_2 + 27u_0^2u_3 - 2(u_1^2 - 3u_0u_2)^{\frac{3}{2}}}{27u_0^3} < 0$$

holds, It shows that Turing instability occurs.

We use some parameter values are  $r = 0.0002$ ,  $K = 0.01$ ,  $c = 0.45$ ,  $d_1 = 0.1$ ,  $r_1 = 0.3$ ,  $s = 4$ ,  $a = 0.2$ ,  $i = 2$ ,  $K_1 = 0.9$ ,  $K_2 = 8$ ,  $r_2 = 10$ ,  $h = 0.0001$ .

### 4.3 Pattern Formation

In this section, we will examine the system (1)–(3) that is used to create patterns in two-dimensional space with zero-flux boundary conditions. For Figs. (11, 12, 13 and 14), we used the finite difference approach to generate numerical results with MATLAB(2014a) software, and also used the same parametric parameters as in the previous section to determine the starting geographical distributions of each species at random.

Now, we can see in Figs. (11, 12, 13 and 14), how the dynamics of systems are distributed spatially throughout time. We found that when coupling parameters varied, the spatial system’s spatial structure changed over time as well as one parameter’s value. Figures (11 and 12) shows the population distribution in space with well-organized structures. It also shows how, as time  $T$  increases from 10 to 400, the population density of the various population classes becomes uniform throughout the area and Figs. (13 and 14) demonstrates the harvesting effects using a fixed time constant and diffusivity.

Finally, all of these figures show the qualitative differences in the spatial density distribution of the spatial system for each species.

### 5 Discussions and Conclusions

In this work, we analyzed the interactions between free-living, mobile prey and their herbivorous predators in aquatic ecosystems. We have investigated three dimensional plankton fish model with Holling type-II and Holling type-IV functional response. Temporal and spatiotemporal model are discussed in this artical. For the temporal system, we first determine the equilibrium points and bound- edness of the system, and then we examine the stability of each equilibrium point and the Hopf bifurcation condition. It has been shown that the rate of interactions is quite sensitive. Determine the stability of the bifurcating periodic solutions as well (1–5). Under certain situations, the system can allow Hopf bifurcation with a constant harvesting rate, as shown in the Figs. 6 and 7.

Analytically, a system is said to be permanent if it is dissipative (i.e., there is a fixed bounded region such that all the trajectories lie in the region for a sufficiently long time  $t$ ) and uniformly persistent (i.e., there must exist a region in the phase space, at a nonzero distance from the boundary, in which all the population victories must lie eventually). Optimal management of renewable resources is connected to the analysis of population dynamic systems with harvesting constant rate. The appropriate integration

of various harvesting policies in a predator–prey system can debate and suggest a number of topics pertaining to practical hazard in the ecological reality (such as the coexistence of interacting species). From a biological perspective, we may infer that when prey is captured, it gets a chance to consolidate or come together. We may infer from this that the prey tends to use collective defense to thwart its harvest, and that stronger group defense is seen at higher harvesting rates that are comparable to the outcome attained.

We have also examined the analytical and numerical conditions that lead to Turing instability in the spatiotemporal system (see Figs. (8, 9 and 10). Additionally, spot patterns may be seen as the diffusivity coefficient rises (11 and 12). Figures (13 and 14) also show the emergence of a pattern when the harvesting rate is constant.

Since the plankton population is slow, compared to the fish population, which grows much more quickly, it is possible to see the fast-slow dynamics from an other angle. Since people eat a lot of fish, both freshwater and marine, predators are harvesting fish populations for food. This research is crucial in ecological conservation, sustainable management of fisheries, and enhancing our knowledge of how ecosystems react to environmental variations. Such studies are pivotal in securing the long-term sustainability and strength of aquatic ecosystems, as well as the welfare of human communities that rely on them.

**Acknowledgements** The authors would like to express their sincere appreciation to the reviewers for their helpful comments in improving the presentation and quality of the manuscript.

**Funding** This research did not receive any specific grant from funding agencies.

## Declarations

**Conflict of interest** The author declares no conflicts of interest.

## References

- Dhar J, Baghel RS (2016) Role of dissolved oxygen on the plankton dynamics in spatio-temporal domain. *Model Earth Syst Environ* 2(1):6
- Baghel RS, Dhar J (2014) Pattern formation in three species food web model in spatiotemporal domain with Beddington–DeAngelis functional response. *Nonlinear Anal Model Control* 19(2):155–171
- Baghel RS, Dhar J, Jain R (2012) Bifurcation and spatial pattern formation in spreading of disease with incubation period in a phytoplankton dynamics. *Electron J Differ Equ* 2012(21):1–12
- Holt RD (2002) Food webs in space: on the interplay of dynamic instability and spatial processes. *Ecol Res* 17:261–273
- Nath B, Kumari N, Kumar V, Das KP (2019) Refugia and Allee effect in prey species stabilize chaos in a tri-trophic food chain model. *Differ Equ Dyn Syst* 1–27
- Kumar V, Kumari N (2021) Bifurcation study and pattern formation analysis of a tritrophic food chain model with group defense and Ivlev-like nonmonotonic functional response. *Chaos, Solitons Fractals* 147:110964
- Kumari S, Upadhyay RK (2020) Dynamics comparison between non-spatial and spatial systems of the plankton–fish interaction model. *Nonlinear Dyn* 99(3):2479–2503
- Maionchi DO, Dos Reis S, De Aguiar M (2006) Chaos and pattern formation in a spatial tritrophic food chain. *Ecol Model* 191(2):291–303
- Callahan T, Knobloch E (1999) Pattern formation in three-dimensional reaction–diffusion systems. *Phys D* 132(3):339–362
- Baghel RS, Dhar J, Jain R (2012) Higher order stability analysis of a spatial phytoplankton dynamics: bifurcation, chaos and pattern formation. *Int J Math Model Simul Appl* 5:113–127
- Hritonenko N, Yatsenko Y et al (1999) *Mathematical modeling in economics, ecology and the environment*. Springer, Berlin
- Baghel RS (2023) Dynamical behaviour changes in response to various functional responses: temporal and spatial plankton system. *Iran J Sci* 47(2):445–455
- Hastings A, Powell T (1991) Chaos in a three-species food chain. *Ecology* 72(3):896–903
- Huisman G, De Boer RJ (1997) A formal derivation of the Beddington–functional response. *J Theor Biol* 185(3):389–400
- Reddy K, Pattabhiramacharyulu N (2011) A model of a three species ecosystem with mutualism between the predators. *a* 11(22), 12–21
- Upadhyay RK, Banerjee M, Parshad R, Raw SN (2011) Deterministic chaos versus stochastic oscillation in a prey–predator–top predator model. *Math Model Anal* 16(3):343–364
- Upadhyay RK, Thakur N, Rai V (2011) Diffusion-driven instabilities and spatio-temporal patterns in an aquatic predator–prey system with Beddington–Deangelis type functional response. *Int J Bifurc Chaos* 21(03):663–684
- Thakur N (2015) Turing and non-turing patterns in diffusive plankton model. *Comput Eco Softw* 5(1):16
- Upadhyay RK, Naji RK (2009) Dynamics of a three species food chain model with Crowley–Martin type functional response. *Chaos, solitons fractals* 42(3):1337–1346
- Bera S, Maiti A, Samanta G (2016) Dynamics of a food chain model with herd behaviour of the prey. *Model Earth Syst Environ* 2:1–9
- Rai V, Upadhyay RK (2004) Chaotic population dynamics and biology of the top-predator. *Chaos, Solitons Fractals* 21(5):1195–1204
- Zhao M, Lv S (2009) Chaos in a three-species food chain model with a Beddington–Deangelis functional response. *Chaos, Solitons Fractals* 40(5):2305–2316
- Upadhyay RK, Thakur N, Dubey B (2010) Nonlinear non-equilibrium pattern formation in a spatial aquatic system: effect of fish predation. *J Biol Syst* 18(01):129–159
- Baghel RS, Dhar J, Jain R (2012) Chaos and spatial pattern formation in phytoplankton dynamics. *Elixir Appl. Math.* 45:8023–8026
- Dhar J, Baghel RS, Sharma AK (2012) Role of instant nutrient replenishment on plankton dynamics with diffusion in a closed system: a pattern formation. *Appl Math Comput* 218(17):8925–8936
- Misra O, Baghel R, Chaudhary M, Dhar J (2019) Spatiotemporal based predator–prey harvesting model for fishery with Beddington–Deangelis type functional response and tax as the control entity. *Dyn Continuous Discret Impuls Syst Ser A* 26:2
- Baghel RS, Dhar J, Jain R (2011) Analysis of a spatiotemporal phytoplankton dynamics: higher order stability and pattern formation. *World Acad Sci Eng Technol* 60:1406–1412
- Dhar J, Chaudhary M, Baghel RS, Pandey A (2015) Mathematical modelling and estimation of seasonal variation of mosquito

- population: a real case study. *Boletim da Sociedade Paranaense de Matematica* 33(2):165–176
- Das A, Pal M (2019) Theoretical analysis of an imprecise prey-predator model with harvesting and optimal control. *J Optim* 2019:1–12
- Dubey B, Agarwal S, Kumar A (2018) Optimal harvesting policy of a prey-predator model with Crowley–Martin-type functional response and stage structure in the predator. *Nonlinear Anal Model Control* 23(4):493–514
- Chakraborty S, Tiwari P, Misra A, Chattopadhyay J (2015) Spatial dynamics of a nutrient-phytoplankton system with toxic effect on phytoplankton. *Math Biosci* 264:94–100
- Walters C, Christensen V, Fulton B, Smith AD, Hilborn R (2016) Predictions from simple predator-prey theory about impacts of harvesting forage fishes. *Ecol Model* 337:272–280
- Whipple SJ, Link JS, Garrison LP, Fogarty MJ (2000) Models of predation and fishing mortality in aquatic ecosystems. *Fish Fish* 1(1):22–40
- Soudijn FH, Denderen P, Heino M, Dieckmann U, Roos AM (2021) Harvesting forage fish can prevent fishing-induced population collapses of large piscivorous fish. *Proc Natl Acad Sci* 118(6):1917079118
- Upadhyay RK, Tiwari S (2017) Ecological chaos and the choice of optimal harvesting policy. *J Math Anal Appl* 448(2):1533–1559
- Badawi H, Shawagfeh N, Abu Arqub O et al (2022) Fractional conformable stochastic integrodifferential equations: existence, uniqueness, and numerical simulations utilizing the shifted Legendre spectral collocation algorithm. *Math Probl Eng* 2022:1–21
- Badawi H, Arqub OA, Shawagfeh N (2023) Stochastic integrodifferential models of fractional orders and Leffler nonsingular kernels: well-posedness theoretical results and Legendre gauss spectral collocation approximations. *Chaos Solitons Fractals X* 10:100091
- Badawi H, Arqub OA, Shawagfeh N (2023) Well-posedness and numerical simulations employing Legendre-shifted spectral approach for Caputo–Fabrizio fractional stochastic integrodifferential equations. *Int J Mod Phys C* 34(06):2350070
- Maayah B, Arqub OA, Alnabulsi S, Alsulami H (2022) Numerical solutions and geometric attractors of a fractional model of the cancer-immune based on the Atangana–Baleanu–Caputo derivative and the reproducing kernel scheme. *Chin J Phys* 80:463–483
- Springer Nature or its licensor (e.g. a society or other partner) holds exclusive rights to this article under a publishing agreement with the author(s) or other rightsholder(s); author self-archiving of the accepted manuscript version of this article is solely governed by the terms of such publishing agreement and applicable law.